

Supporting Information

Probing the variability in oxidation states of magnetite nanoparticles by single-particle spectroscopy

A. Fraile Rodríguez, C. Moya, M. Escoda-Torroella, A. Romero, A. Labarta, and
X. Batlle

*Departament de Física de la Matèria Condensada, Universitat de Barcelona, 08028 Barcelona,
Spain*

Institute of Nanoscience and Nanotechnology (IN2UB), Universitat de Barcelona

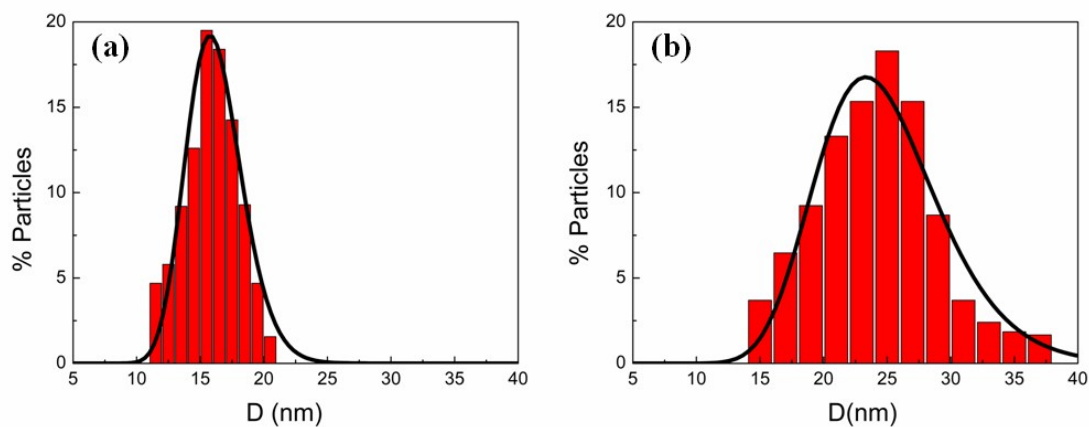


Figure S1. Particle size-distribution for Fe_3O_4 NP. (a) Sample S1, (b) Sample S2.

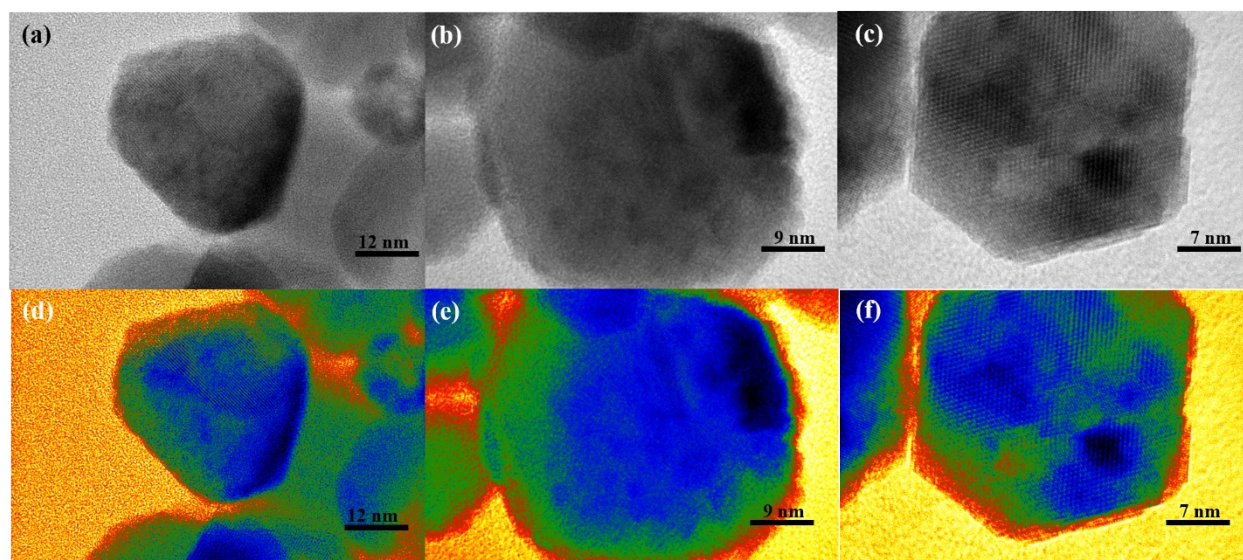


Figure S2. Sample S2 (a)-(c) Gallery of HRTEM images. (d)-(f) The crystallographic domains are outlined with a color contrast.

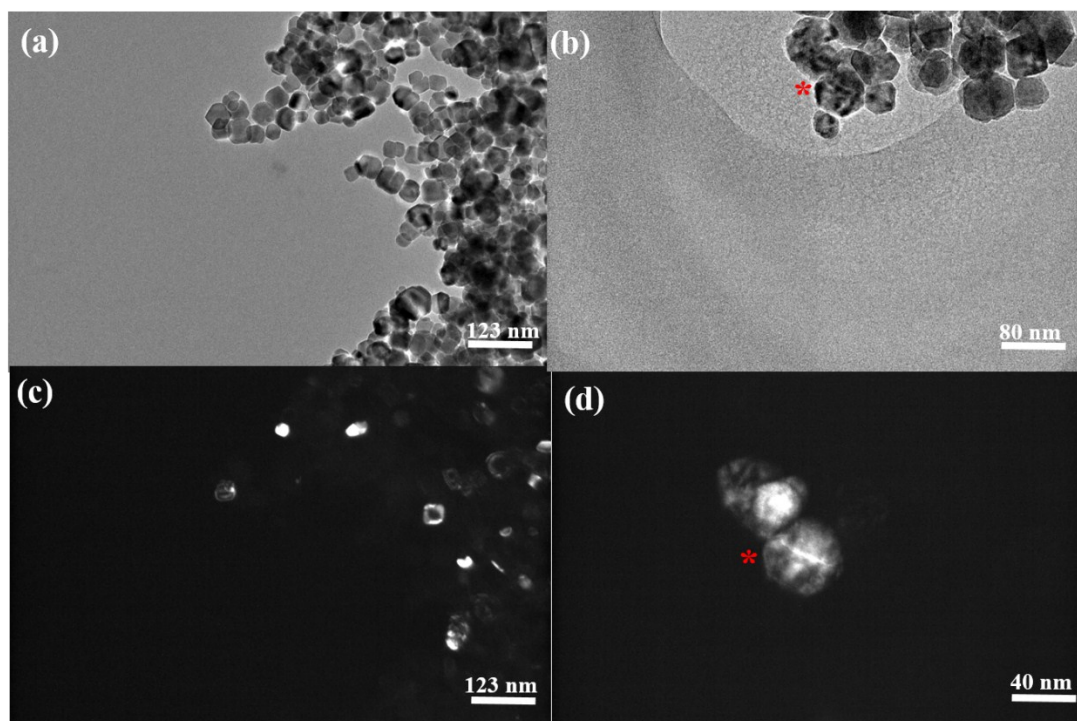


Figure S3. Sample S2. (a)-(b) Low resolution TEM. (c)-(d) Dark field images show NP with structural defects and or/different Fe bases suggested by the different contrast appearing inside the particles.

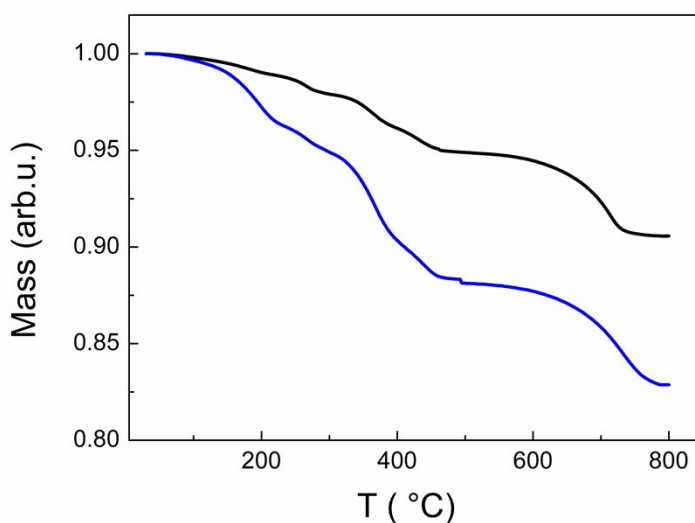


Figure S4. The thermogravimetric (TGA) curves of samples S1 (black line) and S2 (blue line) show the typical two weight-loss plateaus between 200-400 °C and 500-750 °C, that correspond to the removal of both the free oleic acid present in the samples and that attached to the surface of the NP, respectively. The slight weight-loss below 200 °C is attributed to the evaporation of adsorbed water molecules. The total weight-loss is about 9% (S1) and 18% (S2).

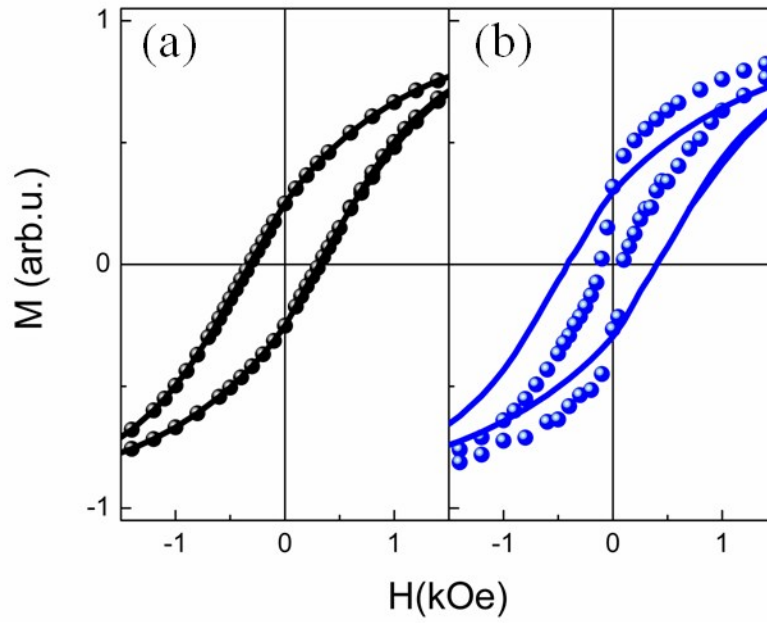


Figure S5. Comparison between the hysteresis loops measured at 5 K before and after field cooling (FC) the samples. Curves are as follows: hysteresis loops before FC for S1 (solid black line) and S2 (solid blue line); and the corresponding hysteresis loops after FC at 10 kOe for S1 (black spheres) and S2 (blue spheres).

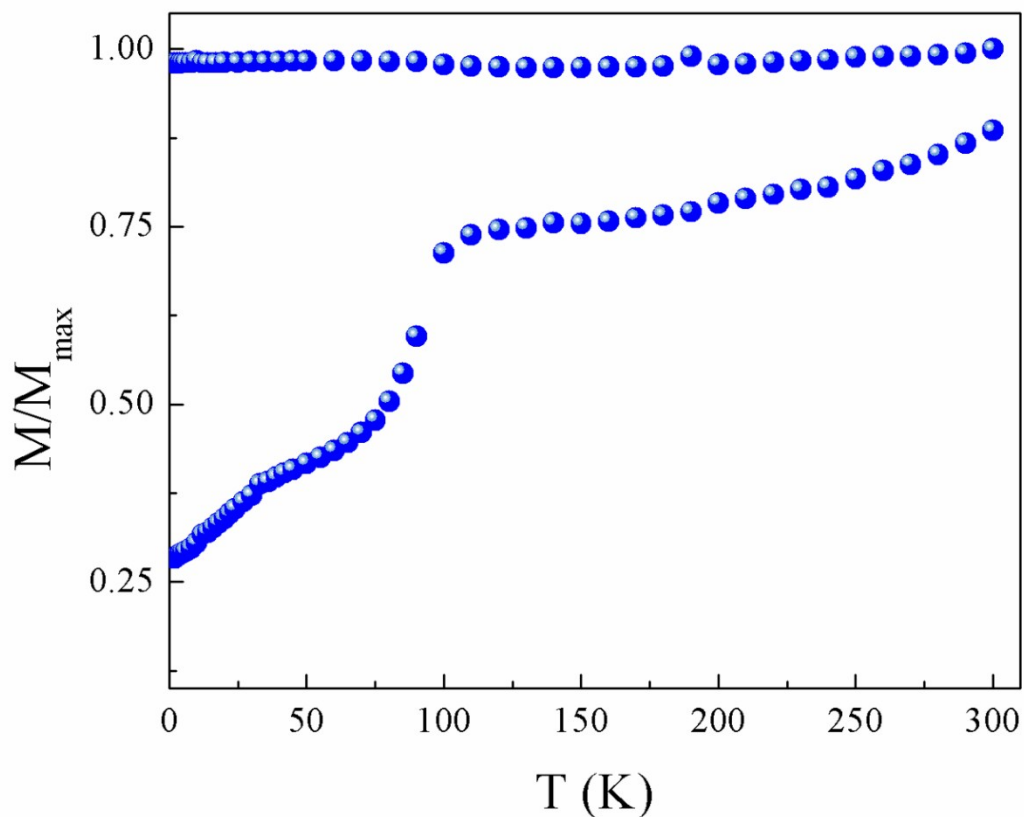


Figure S6. Zero field cooled (ZFC) and field cooled (FC) magnetization curves for sample S2 measured with a Quantum Design SQUID magnetometer from 5 to 300 K with a magnetic field of 50 Oe. The $M_{\text{ZFC-FC}}$ curves show magnetically blocked NP at room temperature. The sharp decrease of the ZFC curve at about 110 K signals de Verwey transition of Fe_3O_4 and confirms the stoichiometry of the sample.

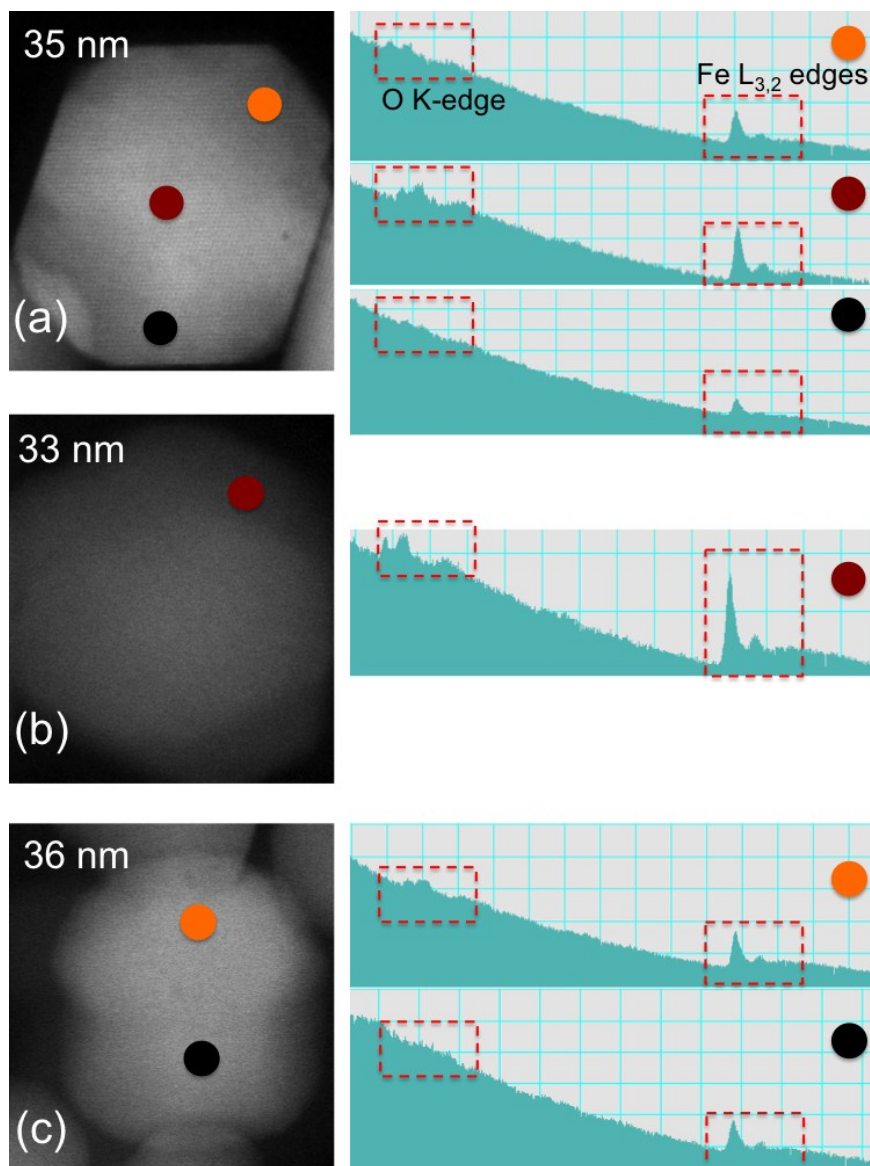


Figure S7. High resolution Scanning Transmission Electron Microscopy (STEM) images (left) and Electron Energy Loss Spectroscopy (EELS, right) of nanoparticles from sample S2 with comparable sizes as those studied by X-ray PEEM. Different contrast in the STEM images are indicative of different iron oxide phases. EELS intensity profiles around the O K-edge and Fe $L_{3,2}$ edges acquired across different locations within the individual nanoparticles confirm that different Fe phases can coexist within the individual particles. Whereas the energy resolution and signal-to-noise ratio are insufficient to distinguish any fine structure in either the $L_{3,2}$ peak shapes or the O pre-edge peak, so as to identify and quantify the iron oxide species in each case, the quenching of the O K-edge peak is an indicative of over-reduced Fe oxide phases (see particles (a) and (c)).